MRC/RUN-0812 : Dust at

Mr Ramjeeawon
Unsolicited proposal
NJ 4/5

Mon. Not. R. Astron. Soc. 000, 000–000 (0000) Printed 29 April 2002 (MN LATEX style file v1.4)

Sensitive VLA observations of Far Infra Red Luminous Quasars

G. K. Beeharry[1] and R. G. McMahon[2]
[1] *Present address: Mauritius Radio Telescope, Department of Physics & Astrophysics, University of Mauritius, Le Réduit, Mauritius*
[2] *Institute of Astronomy, Madingley Road, Cambridge CB3 0HA, UK*
email: rgm@ast.cam.ac.uk, gkb@icarus.uom.ac.mu

29 April 2002

ABSTRACT

Key words: quasars:general - quasars:individual:

1 INTRODUCTION

1.1 The origin of the far infrared emission in z > 4 quasars

The far infrared (FIR; 10-200 μm) emission has been shown, by IRAS, to be very important for starbursts, radiogalaxies and QSOs. The FIR emission makes up for a significant fraction of the total luminosity (up to 95% in many cases e.g. Sanders & Mirabel, 1996).
However, the origin of the FIR emission in QSOs and the most luminous galaxies is an open question. There is mounting evidence that while the FIR emission in radio loud quasars is predominantly of non-thermal origin, in radio quiet quasars and ultra luminous IRAS galaxies it is due to thermal emission from dust (e.g. Sanders et al 1989). The origin of the emission has a wide range of temperatures and distances from the central source (up to ~10kpc). In starbursts the FIR emission is correlated with radio emission (6-20 cm) associated with supernova remnants in the starburst region (e.g. Soifer et al 1987).
Sopp & Alexander (1991) have studied the radio and FIR properties of a large sample of radio loud and radio quiet quasars. They found that the FIR-radio correlation exists in radio quiet quasars and is very similar to the one observed with starburst galaxies and ultraluminous galaxies. Apart from the detection of two gravitationally lensed objects, i.e the Seyfert II-like objects IRAS F10214+4724 (z = 2.28, Rowan-Robinson et al 1991), and the broad absorption line quasar H1413+117 (z = 2.56, Barvainis et al 1995) in the far infrared, there have been no detections of IRAS FIR objects at a redshift > 2. However, the observations at millimetre and sub-millimetre wavelengths (McMahon et al 1994) show that it is possible to observe high redshift (z > 4) objects which emit at FIR in the rest frame.

1.2 BR1202-0725: Dust at z > 4

A major breakthrough was the discovery, by McMahon et al (1994), of 1.2 mm ($\lambda \sim 200$ μm) emission at z=4.69 in a radioquiet quasar of the APM high-redshift QSO survey sample, BR1202−0725. The millimetre emission was interpreted by McMahon et al as being due to dust. This was subsequently supported by submillimetre observations at 450-800 μm by Isaak et al (1994). The 1.25 mm continuum observations were conducted on a sample comprising 5 optically selected QSOs, of which four had z > 4, and 5 radio selected QSOs, including one with z > 4, using the IRAM 30 m telescope. BR1202-0725 was detected at a 4-5 σ level on 3 different occasions and had a flux of 10.5 mJy. Upper limits of $\approx$ 7 mJy were obtained for the rest of the radio quiet quasars. Three of the radio loud quasars were detected. In the case of the radioloud quasars, the millimetre emission was explained as the extrapolation of the synchrotron produced by radio emission. Subsequent observations are described in Beeharry (1997).
The fact that a large amount of dust may have been found at redshifts of z $\geq$ 4 would indicate that heavy element synthesis has already occurred to some extent at this early epoch. Furthermore, the presence of carbon monoxide points to the presence of molecular gas; the essential component of star formation. This shows that the conditions necessary for a star burst to occur were already met in the early universe. Therefore, a starburst is either occurring or has already occurred. In order to test the hypothesis that the FIR emission from the z > 4 quasars is associated with with star formation, sensitive radio observations at other wavelengths are needed. In addition, the high spatial resolution available with the VLA would allow maps of the star forming regions to be obtained at the kiloparsec scale.

Table 1. Objects observed at the VLA

Name	Position (B1950)	Mag (m_R)	z	T^b_{use}
Q0838+359	08 38 07.3 +35 55 21	16[c]	1.77[c]	685
Q0842+345	08 42 30.4 +34 31 41	17[c]	2.12[c]	625
BR0952−011	09 52 27.2 −01 15 53	18.7	4.43	590
1017+279[d]	10 17 07.8 +27 59 07	15.7	1.92	1080
BR1033−032	10 33 51.5 −03 27 46	18.5	4.51	1150
BR1108−074	11 08 41.9 −07 47 45	18.8	3.94	560
BR1114−082	11 14 55.2 −08 22 34	19.7	4.50	555
BR1117−013	11 17 39.4 −13 30 00	18.0	4.00	0[a]
BR1144−072	11 44 02.4 −07 23 25	18.6	4.14	1155
BR1202−072	12 02 49.2 −07 25 50	18.7	4.69	6410
Q1230+162	12 30 39.4 +16 27 26	18.7[e]	0.918	2310
BR1328−043	13 28 55.0 −04 33 26	19.1	4.20	800
BR1335−041	13 35 27.6 −04 17 21	19.4	4.45	845
BR1346−032	13 46 41.1 −03 22 23	18.8	4.01	0[a]
BR1600+072	16 00 54.7 +07 29 16	18.8	4.35	1605

a) Data flagged completely because of interference.
b) Useful time, after flagging interference.
c) Thompson et al 1989, m_V.
d) Control object, m_V.
e) Hewett et al 1991, m_B.

1.3 Radio based study of z > 4 Quasars emitting in the FIR

The optically selected APM high-redshift QSO survey radio quiet z > 4 quasars, detected at 1.25 mm (McMahon et al 1994, Omont et al, 1996), make up a good sample to study the nature of the FIR emission, using the FIR radio luminosity and assuming that the correlation still holds at a high redshift.
Eleven of these objects were selected for observation at the VLA. Five of them had a 3-σ 1.25 mm detection and the flux ranged from 2.8 to 12.6 mJy. They are BR0952-0115, BR1033-0327, BR1117-1329, BR1144-0723 and BR1202-0725.
Omont et al (1996) also made an exploratory programme for millimetre loud radioquiet quasars in the 1-3.5 redshift range. Only one object, Q1230+162, was found. It is a weak lined radio quiet quasar (z = 2.70), having a 1.25 mm flux of 8.6 mJy.
The six above objects were the only ones with z > 2.5 having a firm detection at millimetre/submillimetre wavelengths and it was important to do a deep radio observation of them to explore the FIR radio correlation at weaker levels than had been done until then.
Finally, the set of target objects was completed by including two radio weak quasars which had not been detected at 1.25 mm and two APM quasars which had never been observed previously with the VLA: BR1600+072 and BR1108−074. This information is summarised in Table 1.

2 VLA OBSERVATIONS

2.1 The objects

Given the observational situation, a VLA observation program was set up in order to investigate the possibility that the FIR emission from radio quiet quasars might be due to star formation. This was done under the assumption that the FIR-radio correlation held even at z > 4.
The five radio quiet quasars with z > 4 as well as one with z = 2.70 with firm detections at millimetre and submillimetre wavelengths were included in the observations. These all had 3 σ upper limits, in 20 cm flux, of 0.5 mJy at the VLA. Six control z > 4 objects with similar optical luminosity as well as two lower redshift objects, all with no previous VLA observations at 20 cm, were also observed.

2.2 Expectations and observing strategy

We can use the well established FIR to radio correlation (eg Condon et al 1993) to predict what level of 20 cm radio emission we would expect if the millimetre emission is associated with star formation or more generally, whatever is driving the FIR to radio correlation. This assumes the observed correlation extends a further decade in luminosity.
The median FIR/radio luminosity ratio for $\lambda = 60$ μm is $\sim$ 141 with a dispersion (FWHM) $\pm$ 25. Since most IRAS galaxies have z < 0.1, $\lambda_{observed} \cong \lambda_{rest} = 60$ μm. However, we cannot observe the z > 4 QSOs at $\lambda = 60$ μm; we must estimate the flux.
Using the spectral fit in Figure ??, taken from Isaak et al (1994), the observed flux at 60 μm (rest frame) is $\approx$ 150 mJy. If a FIR (40-120 μm) to radio (20 cm) flux ratio of 141 is assumed, a flux of 1.0 mJy is expected at 20 cm (rest frame). If a spectral index of 0.7 is used, the observed flux at 20 cm would be $(1+z)^{0.7}$ times lower; i.e. 0.3 mJy. Figure ?? shows how this reduction in flux occurs in the spectrum of typical starburst galaxy like M82 (Hughes et al 1990).
Observations carried out at 1 m, corresponding to a rest wavelength of 20 cm at z = 4, lack sensitivity. For instance, the VLA 1 σ rms sensitivity at 90 cm is 1.4 mJy for an integration time of 10 minutes. This is 19.7 times less sensitive than observations at 20 cm. Therefore confusion and integration duration become a serious problem. In addition, 3 dimensional imaging is required to reach this level. Snapshots will not usually reach this level, even with 3 dimensional imaging, as the confusion problem is insoluble with only snapshot (u,v) coverage. The VLA system noise becomes much higher and the available bandwidth is much lower (Perley 1995).
It is *important* to note that this procedure makes *no* assumption whatsoever about any particular cosmological model. Only the rest frame spectral spectral energy distribution is assumed.

2.3 Observations

The radio observations (AM506) were made on the 17th September 1995 using the VLA in the BnA configuration at a frequency of 1.49 GHz (L band). A total of 10 hours of VLA observing time was allocated for this project. The

observing strategy used is now described.
Using these considerations and the fact that the 20 cm VLA sensitivity for a 10 minute integration is 0.071 mJy (Perley 1995), a set of observing times was chosen for each object.
The optically selected APM high-redshift QSO survey radio quiet $z > 4$ quasars, detected at 1.25 mm, and not detected at 8.4 GHz using the VLA (Visnovsky et al 1992), were observed for some 40 minutes (on source) each.
The $z = 4.69$ quasar (BR1202−0725) was observed for a total of some 160 minutes. The rest of the APM $z > 4$ quasars, which had no detection at 1.25 mm, were each observed for a duration in the range of 15-30 minutes.
The one APM $z > 4$ quasar (BR1335−0417), with no previous VLA observation, was observed for 8 minutes.
The quasars in the $1 < z < 3.5$ range were observed using a similar strategy. The $z = 2.70$ quasar (Q1230+1627), which had a previous VLA observation, was observed for some 40 minutes (on source).
The other two, Q0838+359 & Q0842+345, in the same redshift range but having no previous VLA observation, were observed for some 10 mins each.
All the observations which had an integration time of more than about 20 minutes were split up into two or more shorter periods of observing so as to get a better u-v coverage.
3C286 was used as primary calibrator and it was observed at the beginning and near the end of the observing run. Secondary calibrators were observed about every 40 minutes so as to correct for amplitude and phase drifts. The run ended with a secondary calibrator observation.

2.4 Calibration and Maps

2.4.1 Initial processing

The raw scans, from the VLA, of the objects were analysed using the National Radio Astronomy Observatory's (NRAO) Astronomical Image Processing System (AIPS) software package.
The VLA data was first examined using the Aips task TVFLG. This task allows a complete bird's eye view of the whole set of scans. This immediately showed a problem with the data. Out of a total allocation of 10 hours (this includes the dwell time on the sources and the time taken for pointing the telescope), some $3\frac{1}{2}$ hours of dwell time on the sources was corrupted by external interference. This corrupted data was removed. This procedure was carried for both IFs and all the polarisations.
The data was then calibrated using the standard procedures inside Aips.

2.5 Further flagging and raw maps

The whole calibrated data set was examined carefully. All data which looked as if they might contain some interference were completely flagged; i.e. all the baselines were removed. The primary beam is approximately gaussian with a FWHP $30'$ at the observed frequency. Raw unCLEANed large maps ($42' \times 42'$) of the fields were made using Aips task HORUS. These raw maps were thoroughly examined to see whether all the data corrupted by interference had been removed completely. This whole process was carried out for both IFs and circular polarisations. When this procedure of viewing and flagging had been completed, the data was ready to be further processed.

2.6 CLEANing and final maps

The large ($42' \times 42'$) maps made with task HORUS revealed the bright sources ($\gtrsim$ 5 mJy) together with any side lobe which might have been present. The task MX was used to CLEAN in different boxes centered on all the sources contained in the field. Contour plots were made for all the fields mapped.
These maps were examined and smaller maps were plotted so as to look for faint objects. It was found that only two objects had a likely radio counterpart: Q0838+359 and Q0842+345. Their contour plots appear in Figures ?? and ??.
BR1202−0725 was observed for a longer period than any of the other sources. The maps, of different areas and CLEANed to a different extent, of the field centered on the optical position are shown in Figures ?? & ??.
Contour maps for the rest of the sources are shown in figures ?? to ??.

2.7 Analysis of maps: fluxes

The integrated flux, for each of the two objects detected, was calculated using task IMFIT (two dimensional gaussian fit) and their peak flux was computed using task MAXFIT (parabolic fit). Primary beam attenuation has been corrected for, in the estimation of these fluxes, by task PBCOR. The rms noise level for each map was measured using the task IMEAN. An estimate of the rms noise, computed using the formula given in the VLA Observational Status Summary, was also computed for each map. Both these values are listed in Table 2 & in Table 4.

3 DISCUSSION OF THE VLA RESULTS

Out of the 15 objects observed, 2 were detected, useful upper limits were obtained in 11 cases and 2 observations were completely lost because of interference problems. The objects are now examined individually.

3.1 The detected sources

Both detections, Q0838+359 and Q0842+345, come from the group of low redshift ($1 < z < 3.5$) quasars in the Omont et al(1996) sample. In this redshift range, the objects primarily chosen for observation were those which were thought to be strong emitters in the millimetre wavelengths. Omont et al (1996) found that these two objects were tentative detections at the 3 σ level.
Q0838+359 is a bright ($m_V = 16$) weak emission line quasar with a redshift of 1.77 (Thompson et al 1989). Omont et al (1996) report a 1.25 mm flux of 4.50 ± 1.5 mJy. In the present work, a flux of 5.9 mJy is obtained in the 20 cm continuum.
Q0842+345 is an optically bright ($m_V = 17$) broad absorption lines quasar with weak emission lines at a redshift of 2.12 (Thompson et al 1989). We find a 20 cm flux of 1.3

Table 2. RMS of radio source fluxes for detections

Name	Position (B1950)	Measured RMS[a] (μJy)
Q0838+359[b]	08 38 07.3 +35 55 21	90.1
Q0842+345[b]	08 42 30.4 +34 31 41	53.4

a) Using Aips task IMEAN
b) Quasars with no millimetre observations and $1 < z < 3.5$

Table 3. Fluxes of sources detected

Name	Position(B1950)	mm flux[a] (mJy)
Q0838+359	08 38 07.35 +35 55 22.5	4.50 ± 1.5
Q0842+345	08 42 26.72 +34 31 25.1	4.14 ± 1.3

Name	Radio flux (mJy)			
	int.[b]	peak[c]	NVSS int.[d]	NVSS peak[d]
Q0838+359	5.9±0.2	4.7	6.2±0.6	6.7±0.4
Q0842+345	1.3±0.2	1.3	2.5±0.7	4.8±0.5

Name	Radio flux (mJy)	
	FIRST peak[e]	FIRST int.[e]
Q0838+359	5.81±0.15	5.27±0.15
Q0842+345	1.07±0.15	1.70±0.15

a) Flux at 1.25 mm from Omont et al(1996).
b) In this work the integral flux is obtained using Aips task IMFIT, after the primary beam correction.
c) The VLA peak flux is obtained using Aips task MAXFIT.
d) The NVSS position is 3.8″ arcsecs away.
e) The FIRST position is 8.8″ arcsecs away.

mJy.
Q0838+359 and Q0842+345 are both detected in the NVSS survey (D configuration), where the synthesized beamwidth is 44 arcsecs (Perley 1995), at slightly higher flux. Either this difference may stem from the use of the VLA in the B and D configurations of the VLA or the sources are resolved at our resolution. In addition, the values for the NVSS fluxes, extracted from the NVSS catalog on the 6th February 1996, differ from those obtained from the present version of the catalog (11.07.96). The sources may have varied between the epochs of observations. Their fluxes from the FIRST survey (B configuration with a synthesized beamwidth of 3.9 arcsecs, Perley 1995) data are 5.81±0.15 and 1.07±0.15; in very good agreement with the values found in this work (our observations were conducted in the BnA configuration). Unfortunately, the precise epochs of the NVSS and FIRST are unavailable. The situation is complicated since a map may be produced from individual snapshots taken a year or more apart. All the flux values are given in Table 3.
The two detections at 20 cm, Q0842+345 & Q0842+345, are both from the $1 < z < 3.5$ redshift range. Both are weak emission line quasars but Q0842+345 has broad absorption lines as well. If their detections at 1.25 mm are genuine, then both objects seem to have a flat radio spectrum. Observations at 6 cm will shed more light on this matter. If the 6 cm flux shows that the radio spectral index is steep, this would support the view that the spectrum shows an excess in the millimetre band. Soifer et al (1987) find that in the quasars having a flat spectrum in the radio wavelength, the spectrum continues smoothly from the radio through the infrared into the visible regions and say that there is circumstantial evidence for the infrared emission to be predominantly non thermal in origin. In addition, it seems that the luminosities of these quasars are systematically higher by an order of magnitude than those with steep radio spectra and the radio quiet quasars.

Table 4. Upper Limits of radio fluxes and mm fluxes for non detections in radio (20 cm)

Name	Position (B1950)	Theo. rms[a] (mJy)	Up. Lim.[b] (mJy)	S_ν(20cm) (mJy)
BR0952−011[e]	09 52 27.2 −01 15 53	0.060	0.39	0.161
1017+279[h]	10 17 07.8 +27 59 07	0.080	0.17	-0.034
BR1033−032[e]	10 33 51.5 −03 27 46	0.055	0.30	0.039
BR1108−074[h]	11 08 41.9 −07 47 45	0.079	0.43	-0.132
BR1114−082[f]	11 14 55.2 −08 22 34	0.080	0.36	-0.133
BR1117−013[e]	11 17 39.4 −13 30 00	0.053	–	–
BR1144−072[e]	11 44 02.4 −07 23 25	0.058	0.65	0.394
BR1202−072[e]	12 02 49.2 −07 25 50	0.023	0.24	0.004
Q1230+162[g]	12 30 39.4 +16 27 26	0.063	0.28	-0.196
BR1328−043[f]	13 28 55.0 −04 33 26	0.067	0.07	-0.050
BR1335−041[e]	13 35 27.6 −04 17 21	0.096	0.31	0.032
BR1346−032[f]	13 46 41.1 −03 22 23	0.096	0.31	–
BR1600+072[h]	16 00 54.7 +07 29 16	0.054	0.21	0.019

a) At 20 cm, L band, Rms sensitivity(10 min) = 0.071 mJy (BW 50 MHz, 27 Antennas, one IF pair, natural weighing).
b) Using Aips task IMEAN. The limits on the flux values are at the 2 σ levels of the rms noise.
c) Using Aips task Imval. Within 1 arcsec of the optical position.
d) Fluxes and upper limits at 1.25 mm from Omont et al.
e) Quasars with millimetre detections and $z > 4$
f) Quasars with millimetre upper limits $\sigma < 1.5$ mJy and $z > 4$
g) Quasar with millimetre upper limits $\sigma > 1.5$ mJy and $z > 4$
h) Quasars with no millimetre observations and $z > 4$

3.2 The non detections

The $z > 4$ APM sample is now considered. The results are summarised in Table 4. The upper limits of the flux, measured at a distance less than 1 arc second from the optical positions, are also given. The average of these upper limits is 0.16 mJy.
BR1202-0725 is the most studied object of the Omont et al sample. It is a weak emission line redshift $z = 4.69$ quasar with $m_R = 18.7$. McMahon et al (1994) reported a 1.25 mm flux of 10.5 ± 1.5 mJy while Omont et al (1996) report a value of 12.59 ± 2.28 mJy. A 6 cm flux of 0.3 ± 0.2 mJy is given by McMahon et al (1994). Isaak et al (1994) conducted observations of this object in the submillimetre band. It was detected at 1100 μm (21 ± 5 mJy), 800 μm (50 ± 7 mJy) and 450 μm (92 ± 38 mJy).

BR0952-0115 (m_R = 18.7 and z = 4.43) has been observed three times by Omont et al (1996) and has a 1.25 mm flux of 2.78 ± 0.63 mJy. It is a weak emission line quasar.
BR1033-0327 is a weak emission line redshift z = 4.51 quasar with m_R = 18.5. Its 800 μm flux is given as 12 ± 4 (3 σ level) by McMahon et al (1994). Omont et al detected it on three different occasions. Its 1.25 mm flux is 3.45 ± 0.65 mJy.
BR1108-074 (z = 3.94) has not been observed in the millimetre or submillimetre band. It has been included in the exploratory sample of the present observation.
BR1114-082 is a weak emission line z = 4.50 quasar with m_R = 19.7. It has no millimetre or submillimetre observations and has a 1.25 mm flux upper limit of $\sigma > 1.5$ mJy.
BR1144-0723 is a broad absorption line quasar of redshift 4.14 and m_R = 18.8. It has been detected at 1.25 mm with a flux of 5.85 ± 1.03 mJy (Omont et al 1996).
BR1328-043 is a strong emission line quasar (z = 4.20 and m_R = 19.1). It is not clearly detected at 1.25 mm (2.7 ± 1.6 mJy) by McMahon et al (1994). Omont et al (1996) give a 1.25 mm flux of -1.36 ± 1.08 mJy; the tentative detection is not confirmed.
BR1335-0417 has the second highest flux (10.26 ± 1.04) in the 1.25 mm detections in the Omont et al sample. It is a weak emission line quasar with a redshift of 4.45.
There remains the case of the only non detection in the redshift range $1 < z < 3.5$. Q1230+162 is a weak emission line spectrum quasar with z_{em} = 0.918 and m_B = 18.7 (Hewett et al 1991). It has a high luminosity and is the source with the weakest optical emission lines of the LBQS survey. Its redshift is 2.70. It was not detected at 8.4 GHz with a 3 σ upper limit of 0.24 mJy (Visnovsky et al 1992).
Radio quiet quasars are rather difficult to study in the radio wavelengths compared to radio loud quasars because of the comparatively much lower flux.
The majority of the quasars (8) observed in the present work have a weak emission line spectrum. Two have broad absorption lines. One has both a weak emission lines and broad absorption lines. One has strong absorption lines. The IRAS FSC II catalogue does not contain any object in the vicinity of either object. This may mean that IRAS was not a sufficiently sensitive instrument to probe at faint infrared fluxes. More sensitive infrared instruments are needed to investigate this point.
The APM z > 4 quasar sample contains a large variety of quasar types but has no radio (20 cm) detections. The result of this study seems to indicate that the quasars observed in this work are radio quiet with typically $S_\nu \lesssim 10$ mJy rather than radio loud where typically $S_\nu \sim 1$ Jy. This is an *important* result as it would tend to confirm that the far infrared emission in radio quiet quasars may be thermal in origin (Sanders et al 1989).
In the picture provided by the Barvainis et al study (1996), this would tend to indicate that the contribution from the circumnuclear starburst is predominant; this would explain the presence of large amounts of both dust and molecular gas in the dusty quasars (McMahon et al 1994).
In addition, synchrotron emission from the extended component driven by the nucleus and that from the compact VLBI core would have to be absorbed and reprocessed to a great extent. Chini et al (1989) and Andreani et al (1993) find that a non thermal self absorbed synchrotron emission is unlikely. Very deep radio observations of these dusty quasars, so as to increase the sensitivity by a significant amount, may settle this issue.

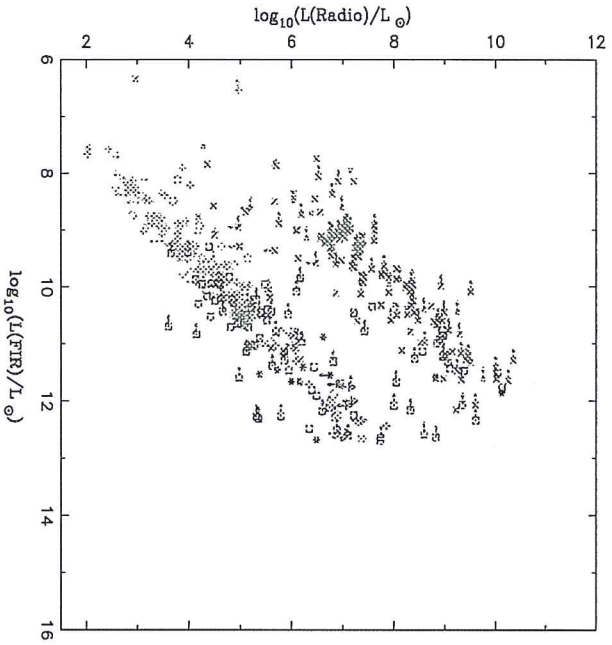

Figure 1. This figure shows the correlation between radio and far infrared luminosities and comes from Sopp & Alexander (1991). Both radio and far infrared luminosities are defined by $L = 4\pi\nu S_\nu D^2$, with ν = 5 GHz for the radio data and ν = 5 THz for the FIR data and D being the luminosity distance. The luminosity is in units of solar luminosity ($L_\odot = 3.8 \times 10^{26}$ W). Each class of objects is represented by a different symbol; late-types by green '+', Seyferts by cyan 'o', radio galaxies by magenta 'x', quasars by gray squares, ultraluminous IRAS galaxies by blue '*'. The high redshift radio quiet quasars, in this work, are represented by red triangles while the low reshift quasars are represented by orange circles with a cross inscribed.

3.3 An extension to the far infrared radio correlation

We now discuss the results in the context of the FIR radio correlation.
The results of observations from this work are shown in Figure 1, an extension of Figure 1 from Sopp & Alexander (1991). The high redshift APM radio quiet quasars, having been observed both at 20 cm and at 1.25 mm, are represented by the orange triangles. The monochromatic luminosity is defined by $L = 4\pi\nu S_\nu D^2$, with ν = 5 GHz for the radio data and ν = 5 THz for the FIR data. The luminosity distance is given by (e.g. Weinberg 1972) $D = \frac{c}{H_o q_o^2}(1 - q_o + q_o z + (q_o - 1)(2q_o z + 1)^{\frac{1}{2}})$. A Hubble constant, H_o = 100 km^{-1} Mpc^{-1} (as in Sopp & Alexander 1991) and an acceleration parameter (q_0) of 1/2 are used.
The flux at 1.25 mm is $\approx$ 230 μm in the rest frame. The flux at 230 μm has been converted to a flux at 60 μm using the spectral energy distribution described in Rowan-Robinson & Efstathiou (1993). The latter give results on the flux emitted at different wavelengths for a spherically symmetric, multi-grain dust model for the far infrared emission of a starburst galaxy. This is shown in Figure ??. By comparing the rel-

ative values of the flux at 60 and 230 μm in the starburst model, a value of the rest frame flux at 60 μm is computed. This value is used in the FIR to radio correlation calculations.

The plot shows two clearly distinct regions. The upper cloud of points contains early-type radio galaxies and radio loud quasars. The lower cloud of points represents the well known far infrared and radio correlation for starburst galaxies (green '+' symbol) which was found to hold (Sopp & Alexander 1991), in addition, for both Seyfert galaxies (cyan 'o' symbol) and quasars (gray square). The data points for the high redshift radio quiet quasars (orange triangle) of this work extend this correlation for higher luminosities. The correlation is seen to hold even for FIR luminosities of $\sim 10^{14}$ $L_{\odot}$ and for radio luminosities of $\sim 10^{9}$ $L_{\odot}$. Sopp & Alexander (1991) found that radio quiet quasars do not occupy the most luminous region of this plot but spanned several orders of magnitude. In the present work, all the data points, except one, extend the lower correlation; the point in the extreme upper right part of the diagram representing BR1202-0725. If it is assumed that the plot shows evidence for a completely separate physical origin for the radio emission in radio loud and radio quiet quasars (cf Sopp & Alexander (1991) and references therein), then the majority of the high redshift APM quasars observed in this work seem to have a spiral-like host galaxy. Supposing that the Lyman alpha absorption system found in the spectrum of BR1202-0725 (Elston et al 1996) is a massive spiral primeval galaxy as kinematic evidence suggested by Lu et al (1996) seems to indicate, then the plot might be interpreted as showing that spiral-like (host) galaxies exist even at very high redshifts. Both the very high redshift and the low metallicity, found in the Lyman alpha absorption system, would tend to indicate that the system may be a very young galaxy.

High redshift galaxies have been found in the vicinity of two of the $z > 4$ APM quasars (Hu et al 1996), BR1202-0725 and BR2237-0607. The galaxies near BR2237-0607 have a moderate luminosity, a strong Lyman alpha emission and a very weak continuum. The authors suggest that this implies that hydrogen depletion has not occurred to a great extent yet. Therefore, substantial chemical enrichment and dust production has not yet taken place. This points to the possible presence of galaxies in their first stage of star formation. These observations may be interpreted to reinforce the hypothesis about the spiral-like host galaxies forming at a redshift $z > 4$.

As these candidate proto-galaxies have been found only in the vicinity of very high redshift quasars, one cannot know whether these are typical galactic objects at these redshifts. However, given the position of the $z > 4$ quasars on the plot, it may be speculated that this is an indication that their host galaxies are spiral-like proto-galaxies.

4 CONCLUSIONS

An investigation of the rest-frame far infrared properties of radio quiet quasars from the $z > 4$ APM quasar sample was undertaken.

Upper limits of ≈ 0.3 mJy were obtained for VLA observations of the sample at 20 cm.

Two detections and one non-detection are obtained in the 1-3 redshift range. The detections have a flux of < 10 mJy while an upper limit of 0.42 mJy (3 $\times$ RMS) is achieved for the non detection.

Combined with previous 1.25 mm observations of the $z > 4$ APM quasar sample (Omont et al 1996), the monochromatic FIR luminosities found are $\sim 10^{14}$ $L_{\odot}$ and the radio luminosities are $\sim 10^{9}$ $L_{\odot}$. These results agree very well with those of Sopp & Alexander (1991), extending their Far Infrared-Radio luminosity plot in the higher luminosity end (Figure 1). The Far Infrared-Radio correlation seems to be valid up to the highest energies achieved up till the present. The $z > 4$ APM radio quiet quasars observed here will be observed for a longer time period so as to obtain their fluxes or at least to lower the upper limits found in this work.

GKB would like to thank the Mauritius Research Council for funds used in buying a computer.

References

Andreani, P., La Franca, F. & Cristiani, S., 1993, MNRAS 261, L35

Barvainis, R., 1996, in *Vistas in Astronomy*, 40, 87-89

Barvainis, R., Lonsdale, C. & Antonucci, R, 1996, Astronom.J. 111, 1431

Barvainis, R., Antonucci, R, Hurt, T., Coleman, P. & Reuter, H.P., 1995, Ap.J. 451, L9

Beeharry, G.K., 1997, PhD thesis, University of Cambridge

Brown, R.L. & Vanden Bout, P.A., 1991, Astronom.J. 102, 1956

Chini, R., Kreysa, E. & Biermann, P.L., 1989, A&A 219, 87

Condon, J.J. & Broderick, J.J., 1986, Astronom.J. 92, 94

Dopita, M.A. & Sutherland, R.S. 1995, ApJ 439, 381-398

Elston, R., Bechtold, J., Hill, G.J., Ge, J., 1996, ApJL 456, 13

Falcke,H., Malkan, M.A., & Biermann, P.L. 1995, A&A, 298, 375

Helou, G., Soifer, B.T. & Rowan-Robinson, M., 1985, Ap.J. 298, L7

Hewett, P.C., Foltz, C.B., Chaffee F.H., Francis, P.J., Weymann, R.J., Morris, S.L., Anderson, S.F., & McAlpine, G.M., 1991, Astronom.J. 101,1121

Hughes, D.H., Gear, W.K. & Robson, E.I., 1990, MNRAS 244, 759

Isaak, K.G., McMahon, R.G., Hills, R.E. & Withington, S., 1994, MNRAS 269, L28

Kellermann, K.I., Sramek, R.A., Schmidt, M., Green, R.F. & Shaffer, D.B., 1994, Astronom.J. 108, 1163

Lacy, M., Miley, G., Rawlings, S., Saunders, R., Dickinson, M., Garrington, S., Maddox, S., Pooley, G., Steidel, C., Bremer, M. N., Cotter, G., Van Ojik, R., Rottgering, H. & Warner, P., 1994, MNRAS 271, 504

Lu, L., Sargent, W.L.W., Womble, D.S., Barlow, T.A., 1996, ApJL 457, 1

McMahon, R.G., Omont, A., Bergeron, J. & Haslam, C.G.T., 1994, MNRAS 267, L9

Omont, A., McMahon, R.G., Cox, P., Kreysa, E., Bergeron, J., Pajot, F., & Storrie-Lombardi, 1996, A & A 315, 10

Perley, R.A., 1995, in *Very Large Array Observational Status Summary*, NRAO

Rawlings, S. 1994, in *The First Stromlo Symposium: The Physics of Active Galaxies*

Rowan-Robinson, M. & Efstathiou, A., 1993, MNRAS 263, 675
Roy, A.L., Norris, R.P., Kesteven, M. J., Troup, E.R. & Reynolds, J.E., 1994, Ap.J. 432, 496
Sanders, D.B., Phinney, E.S., Neugebauer, G., Soifer, B.T. & Matthews, K., 1989, ApJ 347, 29
Sanders, D.B. & Mirabel, I.F., 1996, ARAA 34
Soifer, B.T., Houck, J.R. & Neugebauer, G., 1987, ARAA 25, 187
Sopp H. M., Alexander P., 1991, MNRAS 251, 112
Thompson, D.J., Djorgovski, S. & Weir, W.N., PASP 101, 646, p1065
Visnovsky, K.L., Impey, C.D., Foltz, C.B., Hewett, P.C., Weymann,R.J. & Morris S.L., 1992, ApJ 391, 560
Weinberg, S., 1972, in *Gravitation and Cosmology*, New York, Wiley.
Wilson, A.S., 1995, in *Energy Transport in Radio Galaxies and Quasars Symposium*; ASP Conference Series